Applied Surface Science 321 (2014) 464–468

Contents lists available at ScienceDirect

Applied Surface Science

journal homepage: www.elsevier.com/locate/apsusc

The identification of defect structures for oxygen pressure dependent VO_2 crystal films

Shaojuan Fan[a], Lele Fan[b], Qiang Li[a], Jiandang Liu[a], Bangjiao Ye[a,*]

[a] State Key Laboratory of Particle Detection and Electronics, University of Science and Technology of China, Hefei, Anhui, 230026, China
[b] National Synchrotron Radiation Laboratory, University of Science and Technology of China, Hefei 230029, China

ARTICLE INFO

Article history:
Received 11 June 2014
Received in revised form 13 August 2014
Accepted 12 October 2014
Available online 23 October 2014

Keywords:
VO_2 films with different oxygen content
Phase transition
Positron annihilation technique

ABSTRACT

The defect structures of vanadium dioxide (VO_2) films prepared at different oxygen pressures have been investigated using positron annihilation spectroscopy for the first time. It is found that the concentration of vanadium vacancies is not dependent on oxygen pressure for the range studied, implying that at high oxygen pressure, the point defects which have an effect on transition properties are O-interstitials. The variations of oxygen pressures are more probable to cause changes of the type or concentration of oxygen related defects (such as O-interstitials or O-vacancies) and further influence the transition characters. No matter what kind of the defects they are, the localized point defects have a great impact on the metal-insulator phase transition (MIT) process and the corresponding influence mechanisms are discussed. In addition, the stability of the VO_2 films is also studied. The present results are valuable for the achievement of VO_2-based devices.

1. Introduction

Vanadium dioxide (VO_2) undergoes an ultrafast first-order metal-insulator transition (MIT) near the ambient temperature accompanying significant changes of electrical resistance and infrared transmittance. The transformation is also associated with a structural phase transition from low-temperature monoclinic structure (M-phase), in which VO_2 may be characterized as either semiconductor or a narrow gap insulator, to high temperature tetragonal rutile structure (R-phase), which is metallic [1]. These characteristics make VO_2 a good candidate material for applications in optical switching, memory material, photonics technologies, et al. [2]. However, the MIT behavior of VO_2 can be affected by some factors, such as size, strain, morphology [3–7], and these factors are still not clarified. Therefore, it is necessary to have further studies on the transition behavior of VO_2 for the requirement in applications. Recently, it has been noted that the MIT and electron correlations involved in the phase transition can be affected by the oxygen pressure even if a few percent deviation in stoichiometry can result in several orders of magnitude difference in the phase transition behavior [8–11]. It has been demonstrated that this phenomenon is related to the defects produced by the nonstoichiometry which can nucleate the phase transition [12,13]. However, the specific types of defects induced by the excess or deficient oxygen content are still controversial, and most of results are obtained from the charge neutrality perspective. Some authors think that O or V excess is proposed as the source of V [14–16] or O vacancy [14,17,18], while others suggest the related defects are O [8] or V [15,16,19] interstitial. Therefore, it is of fundamental scientific interest to investigate the specific defects induced by the different oxygen pressures.

Positron annihilation techniques [20] as a unique probe are sensitive and selective to vacancy defects with a sensitivity of 10^{-6} (ppm) order. Performed using a mono-energetic positron beam with variable energy, positron annihilation spectroscopy is well suited to the non-destructive study of defects in thin films. In this paper, the defect structures of VO_2 films at different oxygen pressure are investigated by the Doppler broadening spectroscopy coupled to a slow mono-energy positron beam for the first time. The effect of defects on the MIT behavior of VO_2 films and the corresponding mechanism are discussed. In addition, as vanadium ions have multivalent states, (e.g. V^{2+}, V^{3+}, V^{4+} and V^{5+},) V^{4+} is easily oxidized to V^{5+} in air. In this paper, the stability of the VO_2 films is also studied. The present results are valuable for the achievement of VO_2-based devices.

2. Experimental

VO_2 films were prepared by the pulsed laser deposition (PLD) method on Al_2O_3 (0001) substrate, reported in the literature [21].

* Corresponding author at: University of Science and Technology of China, No. 96, JinZhai Road Baohe District, Hefei, Anhui, 230026, China. Tel.: +86 0551 63606914.
E-mail address: bjye@ustc.edu.cn (B. Ye).

http://dx.doi.org/10.1016/j.apsusc.2014.10.057
0169-4332/

The oxygen partial pressures used for synthetizing samples are 1.6 Pa, 2.3 Pa, 2.7 Pa (the optimal value) and 3.0 Pa, respectively. In addition, other preparation conditions for films remain the same. The structures of VO_2 films were determined by the MAX 18 AHF X-ray diffractometer (XRD) with Cu Kα_1 radiation (λ = 1.54056 Å). The thicknesses of VO_2 films were measured by stylus surface profilometry. X-ray photoelectron spectroscopy (XPS) with Al Kα radiation was employed to investigate the oxidation degree of the surface in the four films. Temperature-dependent electrical resistance was measured by the standard four-probe methods. Doppler broadening spectroscopy coupled to a slow positron beam was carried out to measure the positron-electron momentum distribution using radioactive ^{22}Na isotopes as a positron source.

3. Results and discussion

Fig. 1(a) shows the XRD results at room temperature for the VO_2 films at different oxygen pressures. By adjusting the technological parameters, polycrystalline films grown preferentially along the different crystal orientation can be prepared [22–24]. The peak at 39.84° is assigned to the (020) (JCPDS: 82-0661) plane of the VO_2 films, while the peak at 41.68° is from the sapphire substrate (0006) diffraction. No other diffraction peaks exist in VO_2 film, which indicates that within range of the oxygen pressure, the prepared VO_2 films have pure phase structure (the pure M1-VO_2 phase) and grow with a preferred orientation. In addition, XRD patterns were measured for the samples after staying in air for six months, in order to detect the stability of the VO_2 films. Fig. 1(b) shows that after staying in air for half a year, VO_2 films still kept a preferred orientation, indicating that good quality VO_2 films with high relative density were obtained. The internal structures of samples have not changed from XRD results. Moreover, the tested samples for other experiments were the VO_2 films which had stayed in air for six months. The designations and film thicknesses for the VO_2 films at different oxygen pressures are displayed in Table 1.

Fig. 2 displays the overall core level XPS survey spectra of VO_2 films under different oxygen pressures. Fig. 2(a)–(d) show the Lorentzian–Gaussian dividing peak analysis of O 1s and V 2p peaks for the four films. From the peak position of the V2p$_{3/2}$ and corresponding V-O signal we can get the different V oxidation state, since the binding energy of the V2p$_{3/2}$ core level is dependent on the V cationic oxidation state. Peaks at around 524 eV and 516 eV correspond to the V2p$_{1/2}$ and V2p$_{3/2}$ core levels respectively. After subtracting the Shirley background, both V2p$_{1/2}$ and V2p$_{3/2}$ peaks are a combination of a V^{5+} peak and V^{4+} peak. The $V^{4+}2p_{3/2}$ peak and $V^{5+}2P_{3/2}$ peak are determined at around 515.1 eV and 517.1 eV respectively. These results confirm the oxidized topmost atomic layers of the films with appearance of a V^{5+} state, which is in agreement with reported results previously [10,25].

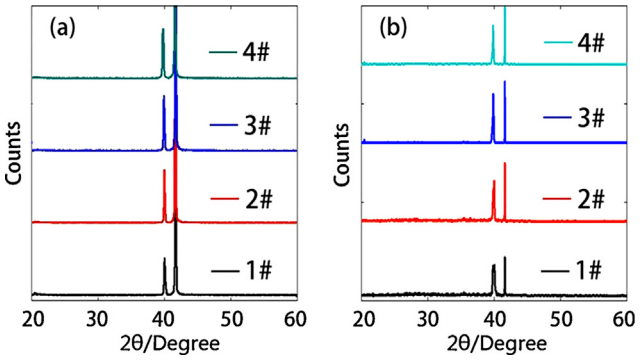

Fig. 1. XRD patterns of (a) VO_2 films prepared under different oxygen pressures and (b) VO_2 films after staying in air for six months.

Table 1
Designations, oxygen pressures, and film thicknesses for VO_2 films and T_{MIT}.

Sample	Oxygen pressure (Pa)	Film thickness (nm)	T_{MIT} (°C)
S1	1.6	164	39.5
S2	2.3	104	41.7
S3	2.7	98	63.0
S4	3.0	107	59.0

The temperature dependences of electrical resistances in VO_2 films are shown in Fig. 3(a). The heating and cooling processes are labeled in the picture. All four films exhibit the thermal hysteresis behavior, and the thermal hysteresis width of the film at oxygen pressure of 2.7 Pa is the largest. It becomes smaller when the oxygen pressure is higher or lower than the optimal oxygen pressure. In addition, the resistance of the M-phase and the onset of the MIT at temperature T_{onset} decrease gradually when the oxygen pressure slightly deviates from the optimal value. Fig. 3(b) is the differential curves which clearly show that the determined transition temperatures of the four films with the oxygen pressure increasing are about 39.5 °C, 41.7 °C, 63.0 °C and 59.0 °C, respectively. Clearly, the transition temperature of film at the optimal oxygen pressure is the largest. The variation trends of T_{onset} and T_{MIT} values for all samples are in correspondence with the phase diagram of VO_2 with low doping concentration developed by Nazari et al. [26]. We assign these dependences to the distinct changes in the localized defects induced by the nonstoichiometry, which will be discussed below.

The results of Doppler broadening spectroscopy coupled to a slow positron beam are displayed in Figs. 4 and 5. Doppler broadening spectroscopy is characterized by S-parameter. S-parameter is defined as the proportion of counts in the central area of the 511 keV annihilation peak. The variations of S parameter as a function of incident position beam energy for the four VO_2 films are shown in Fig. 4 respectively. Positron mean implantation depth in material can be obtained from the semi-empirical formula in literatures [27,28]. Indeed, the slowing down histories of a large number of positrons had been simulated by the VN model which was first proposed by Valkealahti and Nieminen in 1983 [29]. It is found that due to the larger electron scattering in VO_2, the stopping power of VO_2 for positrons is stronger than in Al_2O_3. For example, when the positron inject energy is 7 keV, the mean implantation depths in Al_2O_3 and VO_2 are about 200 nm and 130 nm respectively. S-parameter profile reflects the surface, bulk and substrate of the samples. The variation of S-parameter at low energies ($E < \sim 3.0$ keV) is assigned to positron trapping at the surface of films. Combining the simulation results with the measured thicknesses as shown in Table 1, it can be deduced that for the first sample S1, when positron energies are higher than about 7.5 keV, S-parameter can be mainly attributed to annihilation in the substrate; for the other three samples, S-parameter can be mainly ascribed to annihilation in the substrate when the positron implant energies are larger than about 6.5 keV. All the *S*–*E* curves of the films show a slight change in slope at the film-substrate interface. S-parameter for positron energies between about 3.0 keV and 7.5 keV in S1 mainly reflects the bulk of VO_2 films, while in *S*2–*S*4, the energy range is about 3.0 keV to 6.5 keV, which have been marked in Fig. 4. Fig. 4 shows an *S*-value plateau extending to a little higher energy for each sample, and this may be due to that the *S*-value for the near surface of Al_2O_3 accidently closes to the VO_2 film.

As the surface of films itself is a two-dimensional defect, along with the surface of VO_2 films were oxidized, it results in that the variation of *S*-parameter of the surface differs greatly from the bulk of the VO_2 films. Importantly, *S*-parameter in film layer for the four films did not exhibit any difference for all samples, as shown in Fig. 5(a), and the smooth curves in the figure are the fitting results obtained from VEPFIT. As a reference, the S-parameters

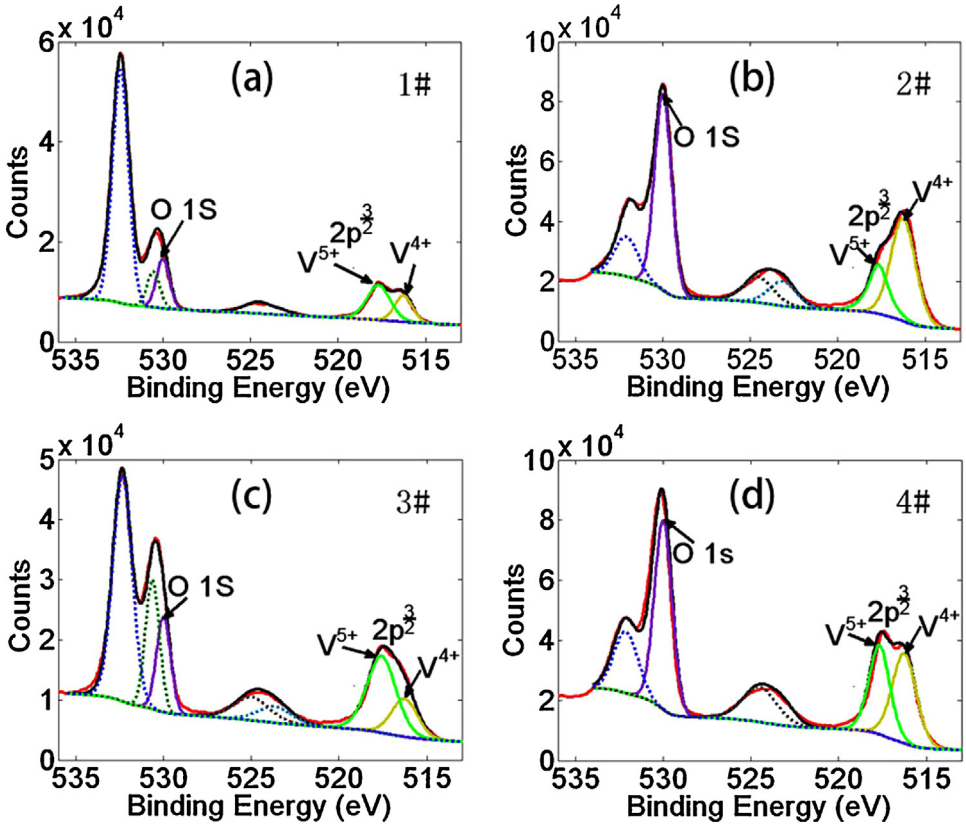

Fig. 2. (a)-(d) XPS spectra of V2p lines and O1s lines with the Lorentzian–Gaussian dividing peak analysis for the VO_2 films.

of a monocrystalline Silicon and a virgin ZnO single crystal which possesses the hexagonal wurtzite structure have been displayed in Fig. 5(b). As V-vacancies are negatively charged, positron is sensitive to detect V-vacancies in films in principle. Therefore, the absence of a variation in *S*-parameter suggests strongly that the concentration of V-vacancies is not dependent on oxygen pressures for the range studied. In fact, films prepared at different oxygen pressures will have different defect conditions. When the oxygen pressure is higher than the optimal value, the potential defects in VO_2 films should be V-vacancies or O-interstitials. As the concentration of V vacancies is invariable, it is implied indirectly that the change of oxygen pressure mainly induces the variation of O-interstitials concentration and hence influences the transition properties. For the films at lower oxygen pressures, the main defects existing in films may be O-vacancies (positively charged) or V-interstitials. As positron annihilation spectroscopy is not sensitive to those defect types, the S-parameter of VO_2 films with oxygen content deficiency mainly reflects the positrons annihilation in bulk of VO_2 films. More experiments are needed to further identify the defects in VO_2 films at lower oxygen pressures. From the calculation of defect formation energy in the literatures [12,30], O-vacancy is much easier to form. Therefore, the most probable point defects present within the films with lower oxygen content are O-vacancies. Accordingly, it can be concluded that the concentration of V-vacancies is independent to oxygen pressures and the variations of oxygen pressures for the range studied are more likely to cause changes of the type or concentration of oxygen related defects (O-interstitials or O-vacancies).

Different defects introduced by nonstoichiometry oxygen content could cause variations in charge carrier type in M-phase [14]. It was reported that in VO_2 films with less oxygen content effective free carriers are electrons for M-phase [14,26], while they are holes for samples with a little more oxygen content than the stoichiometry of VO_2 [8,14,26]. The existing defects in VO_2 films are

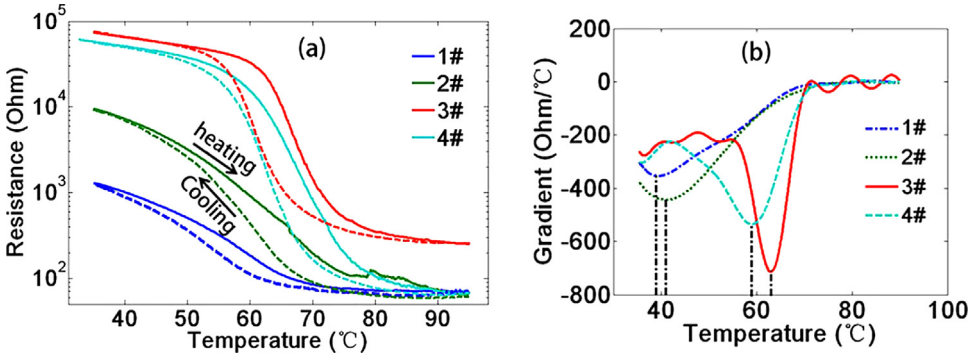

Fig. 3. (a) Temperature dependence of the electrical resistance for the four films and (b) the differential curves used for the determination of the transition temperatures.

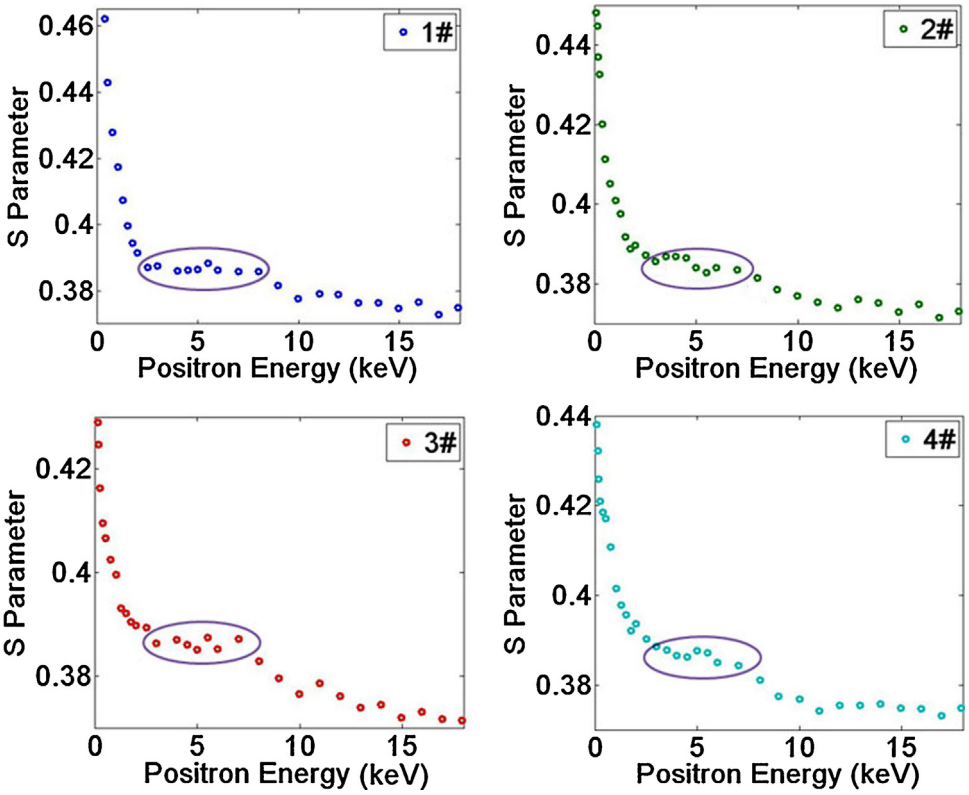

Fig. 4. Low momentum annihilation fraction S-parameter versus incident positron energy E_p for VO_2 films at different oxygen pressures.

correlated with the charge localization, and subsequently affect the band structure. The main features of the VO_2 band structure were qualitatively interpreted by Goodenough [31] and Biermann et al. [32]. The splitting of V^{4+} 3d states induces a gap between empty e_g^{π} band and filled a_{1g} band [30], and the band gap is about 0.7 eV [33]. Additionally, the band gap (E_g) is determined by the variation of localized charge, which depends on the changes of V–V pair twisting and V_d–O_p hybridization [34]. For the films at high oxygen pressures, corresponding defect reaction can be described as follows: $O_2 \Leftrightarrow V_V^{4'} + 4h + 2O_O^X$ [8]. Creating one O-interstitial introduces two hole carries near V^{4+} sites, which could lead to the formation of V^{5+}. As a result, an acceptor level in the band gap above the filled a_{1g} band can be induced and resistance of the M-phase is decreased in VO_2 films with higher O content. While for O deficiency, defect reaction is described as follows: $O_O^X \Leftrightarrow V_O + 2e + \frac{1}{2}O_2$ [34]. The resultant electrons can be trapped by V^{4+} sites to form lower valence states $V^{(4-n)+}$, which could introduce multiple donor levels blow the e_g^{π}, leading to the forbidden gap narrowed and the resistance of M-phase decreased in VO_2 films at lower oxygen pressures. Accordingly, it can be deduced that the defect concentration of O-interstitials or O-vacancies increases with oxygen pressure slightly deviating from the optimal value. In short, all these localized point defects of O-interstitials or O-vacancies induced by the nonstoichiometry oxygen content can introduce hole or electron doping, leading to changes in VO_2 band structure and the drop of resistance in the M-phase.

According to the classical nucleation theory, the nucleation of the phase transition occurs more likely near imperfections such as defects and grain boundaries, where the thermal energy required to overcome the barrier of the transformation is less needed [35–38]. More potent defects can lead to an earlier occurrence of the phase transition. Therefore, defects play an important role during the

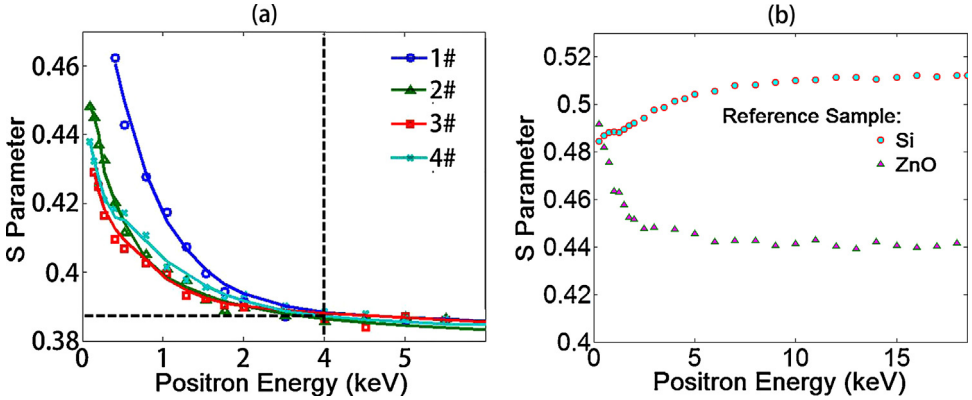

Fig. 5. (a) S-parameters of all films placed together in a figure to compare with each other. The smooth curves are the fitting results with VEPFIT. (b) S-parameters of the reference samples Si and ZnO.

transformation. The dropping resistance between T $_{onset}$ and T_{MIT} is attributed to the onset of the Mott transformation in domains of the films, and the co-existence of a mixed metallic and M-phase [38]. For the mixed phase during MIT, the free electrons from V 3d orbits in the metallic regions will diffuse into the untransformed domain to occupy the V $3d_{||}$ band near the valence state edge [39]. The existence of localized point defects induced by the nonstoichiometry oxygen content can introduce hole or electron doping, leading to the band gap of the M-phase lowing. With point defects concentration of VO_2 films increasing, more "localized" conductivity can be formed. Therefore, defects in VO_2 films promote the onset and progress of the transformation. In the present study, the localized point defects of O-interstitials or O-vacancies act as the initial nuclei sites of the MIT process. The transformation nucleation sites generated by O-vacancies or O-interstitials will reduce the thermal energy required to overcome the barrier of MIT in VO_2 films. As a consequence, the T $_{onset}$ and T_{MIT} of the transformation decrease and thermal hysteresis loop narrows down with the increasing defect concentration, as shown in Fig. 3(a).

4. Conclusions

In conclusion, high quality VO_2 films with a pure M-phase have been prepared by PLD method. After staying in air for six months, VO_2 films still kept a preferred orientation except the film surface was oxidized, indicating good quality VO_2 films with high relative density were obtained. The results of positron annihilation spectroscopy suggested strongly that the concentration of vanadium vacancies is not dependent on oxygen pressures for the range studied. More probably, the variations of oxygen pressures mainly cause the type or concentration of oxygen related defects (such as O-interstitials or O-vacancy) changing. It is proved indirectly that at higher oxygen pressures, the most probable point defects which have an effect on the transition properties are O-interstitials in VO_2 films. According to the calculation of defect formation energy, O-vacancy can be introduced more easily for VO_2 films with lower oxygen content. The variation trends of resistance in M-phase, thermal hysteresis loop, T_{onset} and T_{MIT} across the transformation show substantial defect dependences. The point defects are correlated with electron (hole) localization and subsequently change the band structure. Besides, according to the classical nucleation theory, the local point defects which act as the initial nuclei sites of the MIT process, promote the onset and progress of the transformation. Therefore, the resistance of the M-phase and the values of T_{onset} and T_{MIT} gradually decrease as oxygen pressure slightly deviates from the optimal value. Moreover, the thermal hysteresis loop narrows down as the point defects concentration increases. It should be noticed that elevated defect concentration can reduce the T $_{onset}$ and T_{MIT}, but it accompanies the decrease of the M-phase resistivity, suggesting a weakening of the transformation process. In short, the localized point defects despite the defect types play an important role during the MIT. Moreover, the current experiments results display a useful clue to obtain a deep insight of the transformation mechanism and to optimize the development of VO_2-based devices.

Acknowledgments

This work is financially supported by National Natural Science Foundation of China (Grant Nos. 11175171 and 11105139).

References

[1] M. Marezio, D.B. McWhan, J.P. Remeika, P.D. Denier, Phys. Rev. B 5 (1972) 2541.
[2] Z. Yang, C. Ko, S. Ramanathan, Annu. Rev. Mater. Res. 41 (2011) 337.
[3] J. Jian, A.P. Chen, W. Zhang, H. Wang, J. Appl. Phys. 114 (2013) 244301.
[4] Y.F. Sun, S.S. Jiang, W.T. Bi, R. Long, X.G. Tan, C.Z. Wu, S.Q. Wei, Y. Xie, Nanoscale 3 (2011) 4394.
[5] R. Lopez, T.E. Haynes, L.A. Boatner, L.C. Feldman, R.F. Haglund Jr., Phys. Rev. B 65 (2002) 224113.
[6] J. Narayan, V.M. Bhosle, J. Appl. Phys. 100 (2006) 103524.
[7] D. Brassard, S. Fourmaux, M. Jean-Jacques, J.C. Kieffer, M.A. El Khakani, Appl. Phys. Lett. 87 (2005) 051910.
[8] Q. Yu, W.W. Li, J.R. Liang, Z.H. Duan, Z.G. Hu, J. Liu, H.D. Chen, J.H. Chu, J. Phys. D: Appl. Phys. 46 (2013) 055310.
[9] S. Kittiwatanakul, J. Laverock, D. Newby Jr., K.E. Smith, S.A. Wolf, J.W. Lu, J. Appl. Phys. 114 (2013) 053703.
[10] H.W. Liu, L.M. Wong, S.J. Wang, S.H. Tang, X.H. Zhang, Appl. Phys. Lett. 103 (2013) 151908.
[11] Z. Yang, S. Ramanathan, Appl. Phys. Lett. 98 (2011) 192113.
[12] K. Appavoo, D.Y. Lei, Y. Sonnefraud, B. Wang, S.T. Pantelides, S.A. Maier, R.F. Haglund Jr., Nano Lett. 12 (2012) 780.
[13] J. Jeong, N. Aetukuri, T. Graf, T.D. Schladt, M.G. Samant, S.S.P. Parkin, Science 339 (2013) 1402.
[14] C.H. Chen, Y. Zhao, X. Pan, V. kuryatkov, A. Bernussi, M. Holta, Z.Y. Fan, J. Appl. Phys. 110 (2011) 023707.
[15] C.C.Y. Kwan, C.H. Griffiths, H.K. Eastwood, Appl. Phys. Lett. 20 (1972) 93.
[16] H.T. Yuan, K.C. Feng, X.J. Wang, C. Li, C.J. He, Y.X. Nie, Chin. Phys. Soc. 13 (2004) 0082.
[17] S. Zhang, I.S. Kim, L.J. Lauhon, Nano Lett. 11 (2011) 1443.
[18] E. Kusano, J.A. Theil, J. Vac. Sci. Technol. A 7 (1989) 1314.
[19] C.H. Griffiths, H.K. Eastwood, J. Appl. Phys. 45 (1974) 2201.
[20] F. Tuomisto, L. Makkonen, Rev. Mod. Phys. 85 (2013) 1583.
[21] L.L. Fan, Y.F. Wu, C. Si, C.W. Zou, Z.M. Qi, L.B. Li, G.Q. Pan, Z.Y. Wu, Thin Solid Films 520 (2012) 6124–6129.
[22] L.L. Fan, S. Chen, Y.F. Wu, F.H. Chen, W.S. Chu, X. Chen, C.W. Zou, Z.Y. Wu, Appl. Phys. Lett. 103 (2013) 131914.
[23] K. Nagashima, T. Yanagida, H. Tanaka, T. Kawai, J. Appl. Phys. 100 (2006) 063714.
[24] T.H. Yang, S. Nori, H. Zhou, J. Narayan, Appl. Phys. Lett. 95 (2009) 102506.
[25] C. Ko, Z. Yang, S. Ramanathan, ACS Appl. Mater. Interfaces 3 (2011) 3396.
[26] M. Nazari, C.H. Chen, A.A. Bernussi, Z.Y. Fan, M. Holtz, Appl. Phys. Lett. 99 (2011) 071902.
[27] A. Vehanen, K. Saarinen, P. Hautojarvi, H. Huomo, Phys. Rev. B 35 (1987) 4606.
[28] K.A. Ritiey, K.G. Lynn, V.J. Ghosh, D.O. Weich, M. Mckeown, J. Appl. Phys. 74 (1993) 3479.
[29] S. Valkealahti, R.M. Nieminen, Appl. Phys. A 32 (1983) 95.
[30] J. Paier, C. Penschke, T. Kropp, J. Sauer, 11th European Congress on Catalysis-EuropaCat-XI, Lyon, France, September 1st–6th, 2013.
[31] J.B. Goodenough, J. Solid State Chem. 3 (1971) 490.
[32] S. Biermann, A. Poteryaev, A.I. Lichtenstein, A. Georges, Phys. Rev. Lett. 94 (2005) 026404.
[33] S. Shin, S. Suga, M. Taniguchi, M. Fujisawa, H. Kanzaki, A. Fujimori, H. Daimon, Y. Ueda, K. Kosuge, S. Kachi, Phys. Rev. B 41 (1990) 4993.
[34] C. Chen, Z.Y. Fan, Appl. Phys. Lett. 95 (2009) 262106.
[35] C.N.R. Rao, K.J. Rao, Phase Transitions in Solids, McGraw-Hill, New York, 1978.
[36] R. Lopez, T.E. Haynes, L.A. Boatner, L.C. Feldman, R.F.J. Haglund Jr., Phys. Rev. B 65 (2002) 224113.
[37] A. Frenzel, M.M. Qazilbash, M. Brehm, B.G. Chae, B.J. Kim, H.T. Kin, A.V. Balatsky, F. Keilmann, D.N. Basov, Phys. Rev. B 80 (2009) 115115.
[38] H.T. Kim, B.J. Kim, Y.W. Lee, B.G. Chae, S.J. Yun, Physica B 403 (2008) 1434.
[39] B. Lazarovits, K. Kim, K. Haule, G. Kotliar, Phys. Rev. B 81 (2010) 115117.